Electron transport and pressure coefficients associated with the L_{1C} and Δ_{1C} minima of germanium

C. N. Ahmad and A. R. Adams
Department of Physics, University of Surrey, Guildford, GU2 5XH, Surrey, England, United Kingdom
(Received 16 January 1986)

Hall-effect and resistivity measurements have been made on n-type and ultrapure germanium. The n-type material was characterized by measuring the electron mobility μ_L as a function of temperature down to 100 K at atmospheric pressure. At high pressure, the band structure of germanium becomes similar to that of silicon at atmospheric pressure, making the Δ_{1C} minima accessible to direct electrical investigation. In this siliconlike structure, the electron mobility μ_Δ was found to increase with temperature T from 800 $cm^2 V^{-1} S^{-1}$ at 300 K according to $T^{-2.7}$, indicating that intervalley scattering dominates as in silicon. This contrasts with electron scattering in the L_{1C} minima which is dominated by deformation potential intravalley scattering. An analysis with the values $m_t^* = 0.288$ and $m_l^* = 1.353$ gave intervalley coupling constants of 3.7×10^8 and 2.9×10^8 eV cm^{-1} for the 430-K (LO) and 320-K (LA) phonons, respectively. Having established μ_L and μ_Δ, the resistivity ρ was measured as a function of pressure in ultrapure material at 300 K. It was found to increase exponentially below 25 kbar where the material was n type corresponding to $dE_L/dP = (4.8\pm0.2)\times10^{-6}$ eV bar^{-1}. A p- to n-type transition was observed and beyond 35 kbar, where the material was p type, the resistivity decreased exponentially corresponding to $dE_\Delta/dP = -(2.4\pm0.4)\times10^{-6}$ eV bar^{-1}. With the effective-mass values given above, best overall fit was obtained with $\Delta E_{L\text{-}\Delta} = 0.21\pm0.01$ eV at atmospheric pressure.

I. INTRODUCTION

At atmospheric pressure in n-type material the electrons occupy four ellipsoidal minima at the L_{1C} points at the $\langle 111 \rangle$ boundary. With increasing pressure, however, the energy of the L_{1C} minima increases with respect to the top of the valence band, whereas that of the Δ_{1C} minima decreases. At high pressure the L_{1C} and Δ_{1C} minima cross over making the Δ_{1C} minima the lowest, as in silicon. The electrons transfer to them and thus they become accessible to direct electrical measurements.

Miller and Taylor[1] were the first to measure the pressure coefficient of the L_{1C} minima in germanium. Their resistivity measurements to a pressure of 12 kbar were made at about 400 K to achieve intrinsic conduction. Paul and Brooks[2] later repeated the experiment up to 2.7 kbar pressure using pure single crystals in the temperature range of 298—398 K. Resistivity measurements below 30 kbar were made by Nathan and Paul[3] while p-n junction measurements were made by Jayaraman and Kosicki.[4] As a result of the above measurements it became generally accepted that the pressure coefficient of the L_{1C} minima in germanium is

$$\frac{dE_L}{dP} = 5\times10^{-6} \text{ eV bar}^{-1} .$$

Paul and Pearson[5] studied silicon and found that there the energy gap decreases with pressure with respect to the valence-band maximum at a rate

$$\frac{dE_\Delta}{dP} = -1.5\times10^{-6} \text{ eV bar}^{-1} .$$

In a general review article on germanium and silicon, Paul[6] pointed out that the minima with (100) symmetry (Δ_{1C} or X_{1C}) could have a pressure coefficient anywhere between 0 and -2×10^{-6} eV bar^{-1} and this would apply to the Δ_{1C} minima in germanium. Recent results by Wolford *et al*[7] gave a pressure coefficient for the X_{1C} minima of GaAs of $(1.34\pm0.05)\times10^{-6}$ eV bar^{-1} which supports this view. However Pitt[8] suggested that in order to interpret high-pressure results on III-V compounds values as large as -3.0×10^{-6} eV bar^{-1} may be required.

In 1971 Fletcher and Pitt[9] managed to pressurize single crystals of n-type germanium to about 65 kbar; well above the L_{1C},Δ_{1C} minima crossover, and in 1979 Ahmad, Adams, and Pitt[10] briefly reported measurements of the temperature dependence of the electron mobility in the Δ_{1C} minima obtained at high pressure.

This paper analyzes these results in more detail using recent measurements of the pressure dependence of the electron mobility in the L_{1C} valleys of germanium and the Δ_{1C} minima of silicon. The work is also extended to high-pressure measurements on ultrapure germanium where an n-type to p-type transition is observed both as a function of temperature and of pressure. Analysis of the results enables a determination to be made of the pressure coefficients of both the L_{1C} and Δ_{1C} minima of germanium.

II. EXPERIMENTAL ARRANGEMENTS

The standard Van der Pauw[11] technique was used for both resistivity and Hall-voltage measurements. The high-pressure arrangements used have been described elsewhere.[12] Briefly, a Bridgman anvil system was used and

TABLE I. Summary of electrical characteristics of the samples.

Sample	Orientation	ρ (Ω cm)	n (cm^{-3})	μ_H ($cm^2 V^{-1} s^{-1}$)
No. 1	100	33.5	4.72×10^{13}	3950
No. 2	111	3.7	4.74×10^{14}	3920
No. 3	111	2.3	6.81×10^{14}	3980
No. 4 (INGOT A)	100	~48.3	4.3×10^{13}	3028
No. 5 (INGOT B)	111			

the clover-leaf samples were embedded in an epoxy pressure transmitting medium within a MgO gasket. In this system it is possible to generate some uniaxial stress in the direction of the applied load at low pressures before the gasket is properly gripped by the anvils, therefore both [100] and [111] oriented samples were used. Although uniaxial stress was found to affect some [111] samples no effect of splitting of the [111] minima was observed in [100] oriented samples. In practice, as the pressure was increased, the conductivity in the two types of samples converged and passed through a minimum, as observed by Fletcher and Pitt,[9] indicating that above convergence the pressure system is hydrostatic. The electrical characteristics of the samples used, at atmospheric pressure and room temperature, are summarized in Table I.

The samples were pressurized in the MgO pressure cells as described by Vyas *et al.*[12] The load was increased continuously at a rate of $\simeq$2 kbar per minute, at room temperature, and the resistivity and the Hall voltages were monitored at intervals of 5 kbar. Since the pressure effects in the n-type and intrinsic material are quite different, we deal with the two cases separately.

III. INTRINSIC SEMICONDUCTOR

In an intrinsic semiconductor the density of electrons and holes can be written

$$n=p=(N_C N_V)^{1/2}\exp\left[-\frac{E_g}{2kT}\right], \tag{1}$$

where N_C and N_V are the effective density of states of the conduction and valence bands, respectively, and are related to the density-of-states effective masses m^* by $N=2(2\pi kTm^*/h^2)^{3/2}$. E_g is the band gap. The conductivity then becomes

$$\sigma=ne(\mu_n+\mu_p),$$

where μ_n and μ_p are the effective mobilities of electrons and holes, respectively. From the above equations it follows that

$$\frac{d}{dP}(\ln\sigma)=\frac{1}{2}\frac{d}{dP}[\ln(N_C N_V)]+\frac{d}{dP}[\ln(\mu_n+\mu_p)]-\frac{1}{2kT}\frac{dE_g}{dP}. \tag{2}$$

IV. EXTRINSIC SEMICONDUCTOR

In extrinsic semiconductors most of the charge carriers which take part in conduction are provided by shallow donors or acceptors whose activation energy does not change appreciably with pressure. This was confirmed experimentally for the n-type samples studied here. The intrinsic carriers can be neglected and the main effect of pressure on conductivity is, in this case, the term $d/dP[\ln(\mu_n+\mu_p)]$ of Eq. (2) which further reduces to

$$\frac{d}{dP}\ln\sigma=\frac{d}{dP}[\ln\mu],$$

where μ is the electron or hole mobility for n- or p-type material, respectively.

The mobility of electrons is affected by the application of pressure in a number of ways. In the low-pressure region the effective mass of the electrons increases tending to reduce the mobility while the phonon energy increases tending to increase the mobility. If the pressure is large enough then the electrons may transfer to the higher minima where their mobility may be very different and this redistribution of electrons among the bands gives rise to a change in the average mobility of the electrons. Moreover the mobility of the electrons is further limited due to the enhanced intervalley scattering between nonequivalent valleys when their energy is within a few kT of one another. All these effects can be studied by pressure experiments.

V. EXPERIMENTAL RESULTS

A. Extrinsic material

The variation of the normalized resistivity, ρ/ρ_0, with pressure for a typical sample is shown in Fig. 1. It is clear from Fig. 1 that the pressure range can be divided into three regions. In the low-pressure region, i.e., up to 10 kbar, the resistivity increases slowly. This is believed to be due mainly to a decrease in the electron mobility within the L_{1C} minima. To avoid the shear stresses described previously which may be present at low pressures, the measurements were repeated to 8 kbar in a liquid-pressure transmitting fluid in a piston and cylinder apparatus and the results for the mobility variation are shown in Fig. 2. As one can see the mobility decreases by nearly 5% in 8 kbar.

When only deformation potential scattering is occurring the mobility is expected to depend on the density-of-states effective mass according to $\mu_L \propto (m^*)^{-5/2}$. The pressure coefficient of the direct gap at the L point is 7.5×10^{-6} eV bar^{-1} (Ref. 13) resulting in an increase of the transverse effective mass which can be calculated using $\mathbf{k}\cdot\mathbf{p}$ theory. Assuming the longitudinal effective mass is independent of pressure leads to a rate of increase of the density-of-states effective mass

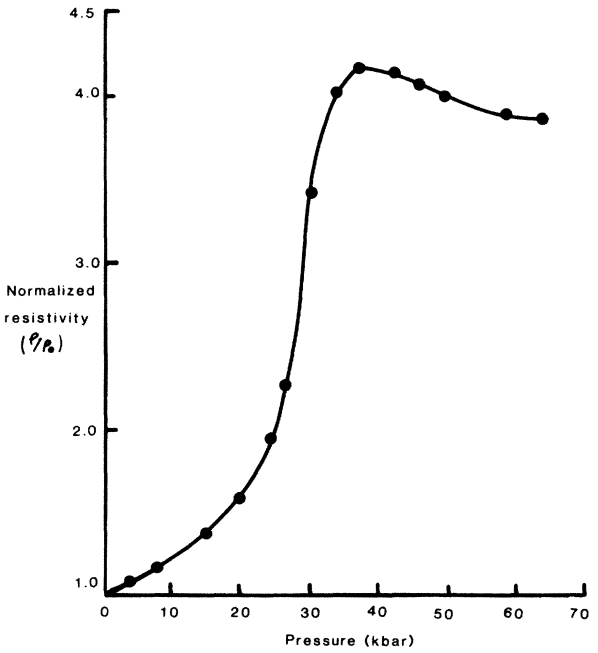

FIG. 1. Normalized resistivity versus pressure for sample No. 1 measured at room temperature.

$$\left[\frac{1}{m^*}\right]\left[\frac{dm^*}{dP}\right]=0.194\%\ \text{kbar}^{-1}\ .$$

This results in the full curve in Fig. 2. As can be seen, this cannot account for all of the change observed and Nathan *et al.*[3] have explained the discrepancy in terms of the thermal transfer of electrons to the Δ_{1C} minima.

In the 20—40 kbar intermediate region, the L_{1C} and

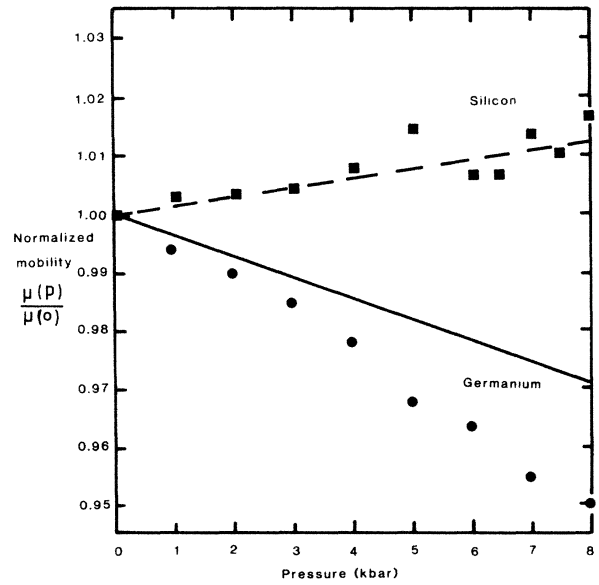

FIG. 2. Variation of electron mobility in the L_{1C} valleys of Ge, ●, and the Δ_{1C} valleys of Si, ■, to 8 kbar at 300 K. Theory for Ge including only deformation potential scattering, ——, and for silicon, – – – –, including intervalley scattering.

Δ_{1C} minima approach one another and nonequivalent intervalley scattering between the two sets of minima increases and, hence, the electron mobility is further reduced. Also electrons transfer from the L_{1C} to the Δ_{1C} minima, where their mobility is about an order of magnitude less, which reduces further the average mobility. All these three processes make the resistivity rise rapidly. The maximum in resistivity at about 33 kbar occurs when most of the electrons have transferred to the low mobility Δ_{1C} minima, but the nonequivalent intervalley scattering between L_{1C} and Δ_{1C} minima is still influencing the relaxation time. These results are in good agreement with those already reported by Fletcher and Pitt.[9]

In the high-pressure region, i.e., above 60 kbar, when the L_{1C} minima have moved a few kT above the Δ_{1C} minima, the electron transfer is complete and the electron mobility, which will be shown to be dominated by intervalley scattering, starts to increase slowly with pressure. For comparison, measurements have been made on *n*-type silicon up to 8 kbar in the liquid-pressure transmitting fluid and the results are shown in Fig. 2. One can see that a mobility increase of between one and two percent is observed to 8 kbar.

The influence of deformation potential scattering in silicon is small and its variation with pressure is negligible since the effect of the increase in effective mass

$$\left[\frac{1}{m^*}\right]\left[\frac{dm^*}{dP}\right]=0.025\%\ \text{kbar}^{-1}$$

is almost exactly canceled by the effect of the increase in density of silicon assuming a compressibility of 1.02×10^{-3} kbar^{-1}. Intervalley scattering was calculated following the analysis of Long[14] and Rode.[15] Its variation with pressure was calculated using the experimental work of Weinstein and Piermarini.[16] This gave $1/\theta(d\theta/dP)=0.2\%$ and -0.1% for the *f*- and *g*-scattering phonons, respectively. The results we derive for the mobility variation are shown by the dotted curve in Fig. 2 which is in reasonable agreement with experiment.

The normalized Hall constant, R_H/R_{H_0}, and Hall mobility, μ_H/μ_{H_0}, to 65 kbar are shown in Fig. 3. The Hall constant passes through the characteristic band-transfer maximum near the band crossover. This effect has already been observed in GaAs by Pitt and Lees.[17] The return of the Hall constant to its original normalized value by 65 kbar implies that the electron transfer is complete without any carrier loss to deep-lying impurity levels which might exist below the Δ_{1C} minima.

At 65 kbar, when the Δ_{1C} minima are the lowest, the load was kept constant and the resistivity and Hall voltage were monitored as a function of temperature. Figure 4 shows the variation of electron mobility in the Δ_{1C} valley with the temperature down to 100 K. Above 200 K, where the mobility is dominated by phonon scattering, there is good agreement between the samples, indicating the effectiveness and reliability of the epoxy pressure transmitting system. The divergence below 200 K could be attributed, as will become evident from the analysis, to the varying amount of impurity scattering present. For comparison the variation with the temperature of the elec-

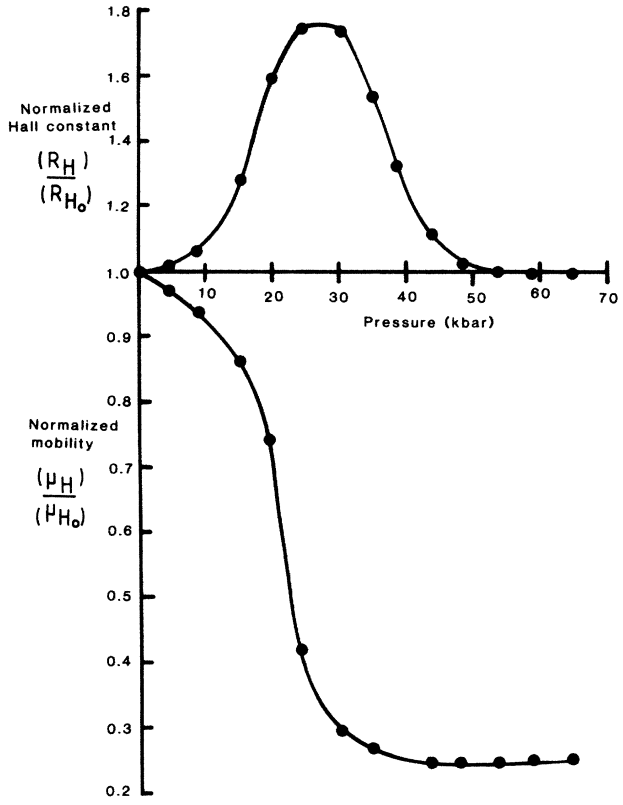

FIG. 3. Normalized Hall constant (R_H/R_{H_0}) and mobility (μ_H/μ_{H_0}) versus pressure for sample No. 1 measured at room temperature.

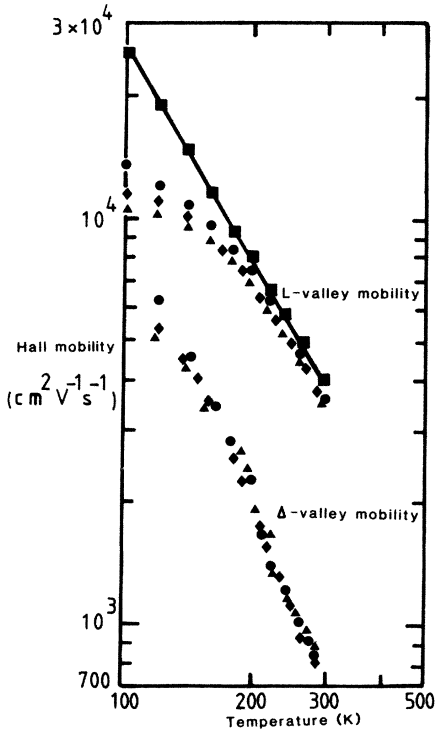

FIG. 4. Measured Hall mobilities in the L_{1C} and Δ_{1C} valleys of Ge Experimental results: ■, Debye and Conwell's sample 55; ●, No. 1; ♦, No. 2; ▲, No. 3; ——, theory.

tron mobility in the L_{1C} valleys is also shown in Fig. 4. This was measured at atmospheric pressure in the same samples.

B. Intrinsic material

Ohmic contacts to the ultrapure material were achieved by implanting As^+ ions $(1\times10^{15}\ cm^{-3})$ to small areas on the periphery of the clover-leaf lobes. The samples were then laser annealed using a multimode Q-switched ruby laser $[E=0.7\ J\,cm^{-2}$ and pulse length 25 ns]. Gold tin was then evaporated and the samples were thermally annealed. Gold wires were attached using a pulse tip bonder for external electrical connections. The rest of the sample preparation is the same as described earlier.

The measured resistivity with pressure for both [100] and [111] oriented samples is shown in Figs. 5 and 6, respectively. Although the density of electrons remains always equal to the density of holes, at low pressure the sign of the Hall voltage corresponded to electron conduction since the electron mobility in the L_{1C} minima of Ge is greater than the hole mobility, i.e., $\mu_L > \mu_p$. At high pressure the Hall voltage changes sign simply because $\mu_p > \mu_\Delta$. To check the role of uniaxial stresses in the solid medium, at low pressure, one of the [100] samples was also pressurized using the piston and cylinder system where pressure can be monitored very accurately. The results, as one can see from Fig. 5, agree very well to the maximum available pressure of 15 kbar. There is a slight indication of splitting in the results of [111] oriented samples, but as the pressure is raised the system becomes hydrostatic in nature. It should be noted that different samples show different degrees of extrinsic conduction.

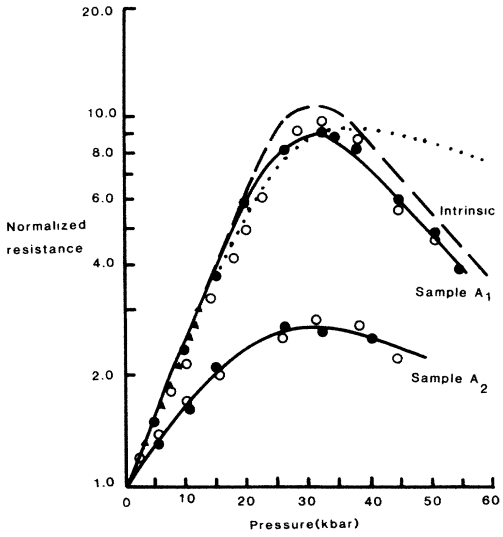

FIG. 5. Normalized resistance versus pressure of high-purity Ge(100) samples measured at room temperature: ○, ●, experimental results (solid medium); ▲, experimental results (liquid medium); ————, pure intrinsic with revised pressure coefficients; ——, theoretical fits to samples obtained by adding the appropriate amount of extrinsic conduction (Table VI); · · · ·, theory using earlier pressure coefficients.

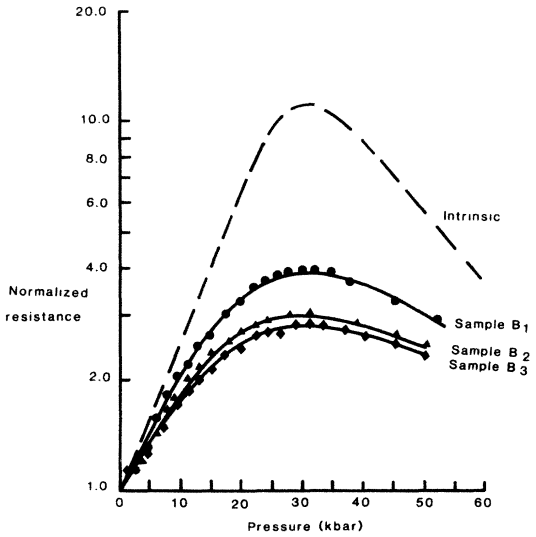

FIG. 6. Normalized resistivity versus pressure of high-purity Ge(111) samples measured at room temperature: ●, ♦, ▲, experimental results; ———, theory for pure intrinsic conduction with revised pressure coefficients; ——, theoretical fits to samples obtained by adding the measured amount of extrinsic conduction, see Table VI.

VI. BAND PARAMETERS

Since the L_{1C} valleys form the conduction-band edge at atmospheric pressure their parameters are well known. The transverse and longitudinal effective masses of electrons at the four equivalent L_{1C} points were obtained from the cyclotron resonance experiments of Dresselhauss *et al.*[18] as $m_t=0.082m_0$ and $m_l=1.58m_0$ at 4 K. These results are in good agreement with the more recent magnetophonon measurements by Eaves *et al.*[19] of $m_t=0.086m_0$ and $m_l=1.52m_0$ measured from 60–270 K with no apparent temperature dependence. Either set yields $m^*=0.22m_0$ which we have used here and assumed to be temperature independent. The intervalley deformation potential E_1 is given by Debye and Conwell[20] as 9.4 eV. This agrees well with the value of $E_1=9.0$ eV determined by Rode[15] from a theoretical fit to the experimental mobility results of Morin[21] and Debye and Conwell.[20] Fawcett and Paige,[22] however, give a value of $E_1=12$ eV which is rather high and in the formulation used here yields a lattice limited mobility 43% less than the measured electron mobility at room temperature.

The electron effective masses in the Δ_{1C} minima in germanium are not known. But Fawcett and Paige,[22] as a result of high-field calculations, predicted effective-mass values of $m_t=0.288m_0$ and $m_l=1.353m_0$. Due to these increased effective masses in the Δ_{1C} minima, Fawcett and Paige[22] found that the acoustic deformation potential has to be reduced from a value for silicon of 8.0 to 3.61 eV in germanium in order to maintain agreement with the experimental results.

The symmetry and polarization of phonons, i.e., longitudinal, optical, or acoustical, involved in intervalley scattering processes are given by group theory. The group selection rules, as discussed by Lax *et al.*,[23,24] and by Streitwolf[25] in general, and by Herbert *et al.*[26] for Ge and Si in particular, restricts the phonons involved in intervalley scattering to those listed in Table II.

The nonequivalent intervalley scattering in germanium has already been studied by Fletcher and Pitt.[9] So in this study we concentrate on the equivalent intervalley scattering in the L_{1C} and Δ_{1C} valleys of germanium.

At low field the electrons in the L_{1C} valley are subject to the following scattering processes:

(i) intravalley acoustic modes,

(ii) intravalley nonpolar optical mode,

(iii) equivalent intervalley scattering between the (111) valleys, and

(iv) ionized impurity scattering.

Intravalley scattering occurs through single-ionized impurities, by transverse and longitudinal acoustic modes of long wavelength, and by nonpolar optical modes. Intervalley scattering, on the other hand, is induced, as described earlier, by LA and LO phonons of similar energies. Thus the nonpolar optical-mode scattering and intervalley scattering could be combined and assumed to occur through a single phonon of energy equivalent to 382 K. This phonon energy was also used by Rode[15] and has been taken from the dispersion curves given by Brockhouse and Iyenger[27] at the (111) zone boundary.

The electrons in the Δ_{1C} valleys are assumed to be subject to the same scattering processes as those in the L_{1C} valleys as listed above but with two exceptions. Firstly, nonpolar optical scattering becomes negligible (Harrison[28]) and secondly, since the Δ_{1C} minima do not lie at the zone boundary the equivalent intervalley scattering will have two components, namely f and g scattering, as discussed by Long.[14] We have adopted Long's approach

TABLE II. Phonons allowed in intervalley scattering according to group selection rules.

Material	Transition		Phonons
Germanium	$\Gamma_{1C}-L_{1C}$	Nonequivalent intervalley scattering	LA
	$L_{1C}-\Delta_{1C}$	Nonequivalent intervalley scattering	LO + LA
	$L_{1C}-L_{1C}$	Equivalent intervalley scattering	LO + LA
Silicon	$\Delta_{1C}-\Delta_{1C}$	Equivalent intervalley scattering	LA + TO

TABLE III. Band parameters for L_{1C} and Δ_{1C} valleys.

Parameter	L_{1C} valley	Δ_{1C} valley
Effective mass ratio		
m_l	1.588	1.353
m_t	0.082	0.288
Density ($g\,cm^{-3}$)	5.33	5.78
Dielectric constant $\epsilon_0=\epsilon_\infty$	15.98	15.98
Longitudinal sound velocity ($cm\,s^{-1}$)	5.4×10^5	5.4×10^5
Acoustic deformation potential E_1 (eV)	9.0	3.61
Intervalley phonon temperatures (K)	LO + LA 382	LO 430 (g scattering)
		LA 100 (g scattering)
		LO + LA 320 (f scattering)

to find the energies of the phonons involved in intervalley scattering in the Δ_{1C} valleys.

We assumed that the Δ_{1C} valleys in germanium lie at the same k value as those of silicon, i.e., $k=(0.8\text{–}0.9)k_B$, where k_B is the wave number at the X point. Then the intervalley scattering processes are classified into two types: one is the g scattering $(k,0,0)\rightarrow(-k,0,0)$ and the other f scattering $(k,0,0)\rightarrow(0,k,0)$. Since the change in the wave vector of electrons by both scattering processes is larger than the maximum length of the phonon vector which is a half of the unit vector of the reciprocal lattice, each scattering must be an Umklapp process. From geometrical considerations it can be shown that the wave vector of the phonons for g scattering, σ_g, is in the $\langle 100\rangle$ direction and that the vector σ_f for f scattering is only 11° off the $\langle 100\rangle$ direction. Furthermore, it can be shown that σ_g has a magnitude of 0.30 of the maximum in the $\langle 100\rangle$ direction, while σ_f is exactly equal to the maximum in its direction. After establishing the wave vectors of the intervalley phonons, their energies were found from the lattice dispersion curve given by Brockhouse and Iyenger.[27] Although the f-scattering phonons are not quite in the $\langle 100\rangle$ direction we feel that the phonon energies at the (100) zone edge would represent a good approximation to their energies since the phonon spectrum does not change very rapidly with direction in the crystal. A single phonon of energy equivalent to 320 K was therefore taken to represent f scattering since LA and LO phonons have similar energy. The energies for the g scattering phonons were taken 0.3 of the way from the zone center as 430-K LO and 100-K LA phonons. Similar energies of the phonons were also used by Fawcett and Paige[22] in their high-field transport calculations for germanium. The band parameters for both the L_{1C} and Δ_{1C} valleys are summarized in Table III.

VII. ANALYSIS OF RESULTS

In order to analyze the Δ_{1C} mobility variation with temperature in terms of possible scattering mechanisms and also because of the important part played by impurity scattering below 200 K in each sample it is necessary to know, apart from other parameters, the density of ionized impurity scattering centers. To determine this we have measured the electron mobility in the L_{1C} valleys as a function of temperature in the same samples at atmospheric pressure. The results are shown in Fig. 4. It is clear from Fig. 4 that above 200 K there is good agreement between the L_{1C} mobility of different samples, but below this temperature they show varying amounts of impurity scattering. In analyzing these results the density-of-impurity centers present in the samples could be found and used in the subsequent analysis for the Δ_{1C} mobility.

The electron mobility due to different scattering mechanisms can be estimated from the individual theoretical formulae. Except for the intervalley scattering, each mobility can be written (in units $cm^2V^{-1}S^{-1}$) using the parameters of Table III as

L_{1C} valleys	Δ_{1C} valleys
$\mu_d=\dfrac{2.2\times10^9}{[E_1\,(\text{eV})]^2T^{3/2}}$	$\dfrac{3.075\times10^8}{[E_1\,(\text{eV})]^2T^{3/2}}$
$\mu_{ii}=\dfrac{1.846\times10^{18}T^{3/2}}{N_1[\ln(1+b)-b/1+b]}$	$\dfrac{1.238\times10^{18}T^{3/2}}{N_1[\ln(1+b)-b/1+b]}$
$b=\dfrac{4.54\times10^{14}T^2}{n'}$	$\dfrac{9.993\times10^{14}T^2}{n'}$

with n' and N_1 defined as

$$n'=n+(n+N_A)\left[1-\frac{n+N_A}{N_D}\right],$$

$$N_1=2N_A+n\ .$$

For the estimation of intervalley scattering we assume that each valley of the conduction band is spherically symmetric. The average of the lifetime associated with this scattering is approximated by replacing the energy term in Herring and Vogt's formula[29] by $\frac{3}{2}KT$. With this assumption the expression for the intervalley scattering can be written (Toyama *et al.*[30]) as

$$\mu_{iv}\approx\mu_d\left[\sum_i\frac{\omega_i}{\omega_A}\left[\frac{T_{ci}}{T}\right]^{3/2}\frac{(T/T_{ci}+\frac{2}{3})^{1/2}}{\exp(T_{ci}/T)-1}+\frac{(T/T_{ci}-\frac{2}{3})^{1/2}}{1-\exp(-T_{ci}/T)}\right]^{-1}$$

(the last term is zero for $T/T_{ci}\leq\frac{2}{3}$), where ω_A,ω_i measure the strength of coupling of electrons to acoustic and

to the ith intervalley phonons, respectively. T_{ci} is the characteristic temperature of the ith phonon.

The overall mobility, μ_{total}, was calculated using Matthiessen's rule

$$\frac{1}{\mu_{\text{total}}} = \sum_i \frac{1}{\mu_i} .$$

The L_{1C}-valley mobility was analyzed first to find the density of the scattering centers involved in the samples used. For this purpose we have used the results of Debye and Conwell[20] for sample 55 in which the mobility seems to be dominated by the deformation potential scattering down to 100 K, as shown in Fig. 4, indicating that the impurity scattering in this sample is negligible. So by including deformation potential scattering mobility and the intervalley mobility for the L_{1C} valley, treating $\alpha=\omega_i/\omega_A$ as an adjustable parameter, a fit to Debye's sample was obtained as shown by the solid line in Fig. 4. Using the resulting value of α the intervalley scattering mobility in the L_{1C} valley was calculated. By combining the deformation potential scattering and the intervalley scattering, fits to our samples were obtained by introducing an appropriate amount of impurity scattering as shown in Fig. 7. The density-of-impurity scattering centers required for these fits are shown in Table IV. Having established the density-of-impurity centers involved in the L_{1C}-valley mobility, we are in a position to analyze the Δ_{1C}-valley mobility by assuming the same density-of-impurity centers as for the L_{1C} valley and adjusting the scattering rate appropriately for the change of effective mass.

Now for the Δ_{1C} mobility the deformation potential scattering is fixed by the parameters of Table III. The ionized impurity scattering, on the other hand, is fixed by the deduced impurity densities of Table IV. Therefore the only variable left is the intervalley scattering mobility. So by including deformation potential, ionized impurity, and the intervalley scattering, both f and g types, best fits to the measured mobility for our samples were obtained by treating α as an adjustable parameter. The results are shown in Fig. 8. From the resulting α values the intervalley deformation potentials for both the L_{1C} and Δ_{1C} valleys were calculated from Conwell's[31] relation $\alpha=2D_i^2 s^2/E_1^2\omega_i$ and listed in Table V, where D_i is the intervalley deformation potential and s is the sound velocity in the material. It is clear from Fig. 8 that the mobility of electrons in the Δ_{1C} minima of germanium is dominated by intervalley scattering as in silicon.

Now we turn to the intrinsic material. In this the Hall voltage is small and its pressure dependence difficult to measure accurately, also its interpretation is complicated. The conductivity, on the other hand, arises from a relatively simple algebraic sum of the contribution from carriers in each band. Since the Fermi level E_F is far from the band edges at E_L, E_Δ, and E_V, we may write their carrier densities as

$$n_L = N_L \exp - \left[\frac{E_L - E_F}{kT}\right] , \tag{3}$$

$$n_\Delta = N_\Delta \exp - \left[\frac{E_\Delta - E_F}{kT}\right] , \tag{4}$$

$$p = N_V \exp - \left[\frac{E_F - E_V}{kT}\right] . \tag{5}$$

In the case of an intrinsic semiconductor

$$n_L + n_\Delta = p$$

and

$$np = n_i^2 = (n_L + n_\Delta)p . \tag{6}$$

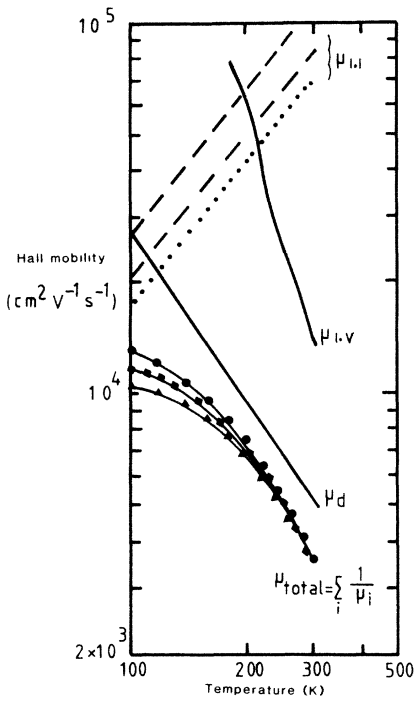

FIG. 7. L_{1C}-valley mobility with individual scattering mechanisms. Each sample has a symbol denoting experimental and; a line denoting theory, i.e., ● and ———, represent sample No. 1; ♦ and —·—·—, represent sample No. 2; ▲ and · · · ·, represent sample No. 3; and, ——, represents the best theoretical fits.

TABLE IV. Density of impurity scattering centers.

Sample	N_D-N_A (cm^{-3})	N_D+N_A (cm^{-3})
No. 6 (Debye and Conwell's sample 55)	1.0×10^{13}	1.09×10^{13}
No. 1	4.72×10^{13}	6.73×10^{15}
No. 2	4.74×10^{14}	1.11×10^{16}
No. 3	6.81×10^{14}	1.36×10^{16}

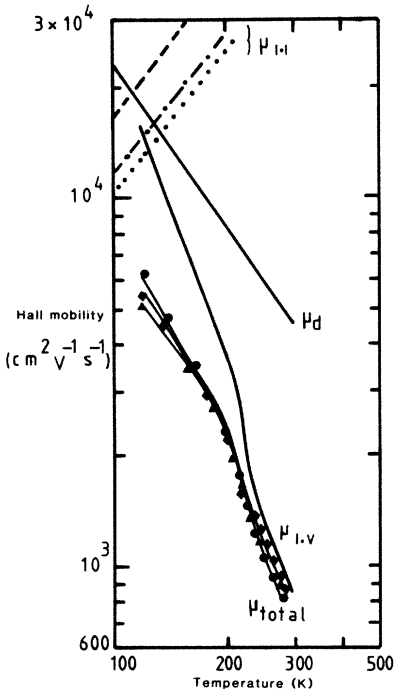

FIG. 8. Δ_{1C}-valley mobility with individual scattering mechanisms. See caption to Fig. 7 for symbol identification. $\mu_{I\text{-}I}$ calculated from $\mu_{I\text{-}I}$ curves shown in Fig. 7.

From Eqs. (3)—(6), taking $E_V=0$, it follows that

$$E_F=-\frac{kT}{2}\ln\left[\frac{N_\Delta}{N_V}\exp\left[-\frac{E_\Delta}{kT}\right]+\frac{N_L}{N_V}\exp\left[-\frac{E_L}{kT}\right]\right] \tag{7}$$

and

$$n_i=n=p=\left[N_L N_V\exp\left[-\frac{E_L}{kT}\right]+N_\Delta N_V\exp\left[-\frac{E_\Delta}{kT}\right]\right]^{1/2} . \tag{8}$$

Assuming density-of-states effective-mass ratios, the Fermi energy, E_F, could be calculated from Eq. (7) and, hence, the carrier densities from (3), (4), and (5). The electrical conductivity

$$\sigma=e(n_L\mu_L+n_\Delta\mu_\Delta+p\mu_p) \tag{9}$$

may be calculated assuming atmospheric pressure values of the mobility $\mu_L=4000$ $\mathrm{cm^2V^{-1}s^{-1}}$, $\mu_\Delta=800$ $\mathrm{cm^2V^{-1}s^{-1}}$ from the last section, and $\mu_p=1900$ $\mathrm{cm^2V^{-1}s^{-1}}$. The hole mobility was assumed to be pressure independent. Recent measurements by Adams and Shantharama[32] have shown that μ_p changes by less than 1% in 8 kbar in all the III-V compounds measured as one might expect from **k·p** theory. The rate of change of conductivity with pressure is given by Eq. (2) where μ_n now represents some suitable average of μ_L and μ_Δ. The results shown in Fig. 2 indicate that the last term in Eq. (2) is dominant. The first two terms are 2 orders of magnitude smaller and are of opposite sign to one another so they tend to cancel below crossover. Equation (2) therefore reduces to

$$\frac{d}{dP}(\ln\sigma)=-\frac{1}{2kT}\frac{dE_g}{dP} . \tag{10}$$

At low pressure when $E_\Delta \gg E_L$ the second term in Eq. (8) becomes negligible and the effective energy gap, E_g, is dominated by E_L so Eq. (10) becomes

$$\frac{d}{dP}(\ln\sigma)=-\frac{1}{2kT}\frac{dE_L}{dP} . \tag{11}$$

At high pressure the converse is true and Eq. (10) becomes

$$\frac{d}{dP}(\ln\sigma)=-\frac{1}{2kT}\frac{dE_\Delta}{dP} . \tag{12}$$

Thus in the very high and very low pressure regions where the variation of $\ln P$ is linear, as shown in Fig. 5, dE_L/dP and dE_Δ/dP can be obtained directly from the gradient without the knowledge of any other parameter.

This analysis holds only for a perfectly pure sample and it was first necessary to establish that no significant extrinsic conduction occurred. To this end the temperature dependence of the Hall mobility was monitored down to 100 K at atmospheric pressure. The mobility variation of one of the samples is shown in Fig. 9. A transition from n-type to p-type conductivity occurred at 150 K. It is interesting to note from Fig. 9 that the transition appears very sharp and the mobility after the transition is similar to that before the transition. This means that the magnitudes of the mobilities of electrons and holes in germanium at 150 K are equal. This is in agreement with the ex-

TABLE V. Intervalley deformation potentials.

Parameter	L_{1C} valley	Δ_{1C} valley		
Phonons (K)	382	430	320	100
α	0.30	1.92	2.21	Negligible
D_i ($\mathrm{eV\,cm^{-1}}$)	3.2×10^8	3.69×10^8	2.94×10^8	Negligible

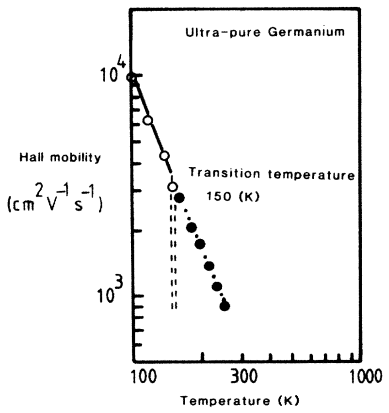

FIG. 9. Variation of measured Hall mobility of carriers with temperature in ultrapure Ge showing a transition from electron, ●, to hole, ○, conduction at 150 K.

TABLE VI. Extrinsic conduction of samples from Ingots A and B (Table I).

Sample	$\Delta\sigma$ ($\Omega^{-1}\,cm^{-1}$)
$A1$	5.96×10^{-4}
$B1$	4.933×10^{-3}
$B2$	7.687×10^{-3}
$B3$	8.723×10^{-3}
$A2$	9.5×10^{-3}

perimental results of Morin and Maita.[33] From the transition temperature at which the Hall mobility goes to zero, the density of electrons and holes, and hence the extrinsic conduction in the sample, were deduced and the results listed in Table VI.

In the case of the most pure sample, $A1$, taking a small extrinsic conduction of $5.96\times10^{-4}\ \Omega^{-1}\,cm^{-1}$ into account and assuming the density-of-states effective-mass ratios in the valence band and L_{1C} and Δ_{1C} minima as $m_V^*=0.40$, $m_L^*=0.56$, and $m_\Delta^*=1.58$, respectively (i.e., $N_\Delta/N_L=4.86$ which gave good agreement between theory and experiment in the last section), best overall fit was obtained, as shown in Fig. 5, resulting in the following parameters

$$\frac{dE_L}{dP}=4.8\pm0.2\times10^{-6}\ \text{eV bar}^{-1},$$

$$\frac{dE_\Delta}{dP}=-2.4\pm0.4\times10^{-6}\ \text{eV bar}^{-1},$$

$$\Delta E_{L\text{-}\Delta}=0.21\pm0.01$$

at atmospheric pressure. This corresponds to $L_{1C}-\Delta_{1C}$ band crossing at 29 ± 2 kbar.

In this analysis of the ultrapure material no account was taken of the increased resistivity due to the enhanced electron scattering between the L_{1C} and Δ_{1C} minima near the band crossover and this may account for the few rather high experimental points near the peak in Fig. 5. To demonstrate the sensitivity of these calculations to the adjustable parameters, the values given by Pitt[8] of $dE_L/dP=5.0\times10^{-6}$ eV bar^{-1}, $dE_\Delta/dP=-1.0\times10^{-6}$ eV bar^{-1}, and $\Delta E_{L\text{-}\Delta}=0.19$ eV at atmospheric pressure, were assumed. The calculated curve is shown dotted in Fig. 5. Although at low pressure the agreement is reasonable, clearly the discrepancy at high pressure is large.

Few samples showed intrinsic conduction, but since the pressure coefficients are deduced from the purest sample, theoretical fits to the less pure samples were obtained simply by taking into account the respective amount of extrinsic conduction determined independently and listed in Table VI. The resultant curves are shown in Figs. 5 and 6 and, as one can see, without any adjustable parameters agreement between theory and experiment is good.

VIII. DISCUSSION AND CONCLUSION

Before we discuss the n type and ultrapure material analysis let us draw the following comparisons from Figs. 4, 7, and 8.

(1) The magnitude of the mobility in the L_{1C} valley of $\simeq4000$ cm^{2}V^{-1}s^{-1} drops to $\simeq800$ cm^{2}V^{-1}s^{-1} in the Δ_{1C} valley.

(2) The gradient of the curve in the L_{1C} valley near room temperature corresponds to $T^{-1.5}$. But the gradient of the Δ_{1C} mobility, near room temperature, corresponds to a $T^{-2.7}$ temperature dependence, similar to silicon at atmospheric pressure. This behavior is typical of the strong intervalley scattering as is evident from Figs. 7 and 8 which list all the scattering mechanisms responsible for limiting the electron mobility in the samples investigated.

(3) The mobility in the L_{1C} valley is dominated by deformation potential scattering at room temperature. Impurity scattering is negligible and the intervalley scattering is small. However, as the temperature is lowered the relative contributions of the ionized impurity scattering and the intervalley scattering changes such that below 200 K the ionized impurity scattering can no longer be ignored although deformation potential remains dominant.

(4) In the Δ_{1C} valleys the mobility is dominated by strong intervalley scattering throughout the whole temperature range. Although the contributions of intervalley and deformation potential scattering are the same from sample to sample and the ionized impurity scattering is fixed from the L_{1C} valley mobility, i.e., there are no adjustable parameters left yet, good agreement with the measured mobility was obtained for each sample throughout the whole temperature range.

The L_{1C} mobility analysis reveals that for an acoustic deformation potential of 9.0 eV we require an intervalley deformation potential of 3.2×10^8 eV cm^{-1} for the 382 K phonon. This intervalley deformation potential agrees very well with 3.0×10^8 eV cm^{-1} calculated by Rode.[15]

The analysis of the electron mobility in the Δ_{1C} valley revealed that for an acoustic deformation potential of 3.62 eV we require an intervalley deformation potential of 3.7×10^8 eV cm^{-1} and 2.9×10^8 eV cm^{-1} for the 430 and 320 K phonons, respectively. These parameters are particularly important for the calculation of high-field transport properties, and are comparable to the calculated values of Fawcett and Paige[22] of 9.5×10^8 eV cm^{-1} and 3.3×10^8 eV cm^{-1} for the 430 and 320 K phonons, respectively. To see the effect of E_1, the acoustic deformation potential, we have used different values and tried to retain the agreement with the experimental data. We find that acceptable agreement with experimental data is confined to a small range of values of E_1, i.e., $3.0\le E_1\le5.0$. For values outside these limits agreement with the mobility temperature variation becomes poor. The corresponding range of the intervalley deformation potential becomes $1.97\times10^8\ge D_1\le3.9\times10^8$ eV cm^{-1} for the 430 K phonon and $2.8\times10^8\le D_2\le3.07\times10^8$ eV cm^{-1} for the 320 K phonon. This range of values for D_i is in good agreement with the silicon values determined by Long.[14] Rode[15] has obtained a value of 3.0×10^8 eV cm^{-1} for silicon and Toyama *et al.*[30] determined a value of 7.0×10^8 eV cm^{-1} for GaP. A negligible coupling constant was found for the low-energy, 100 K phonon in agreement with the results of Rode[15] for silicon and GaP.

In summary we have measured the electron mobility in the L_{1C} and Δ_{1C} valleys of Ge and they were found to vary with temperature according to $T^{-1.5}$ and $T^{-2.7}$,

respectively. From these characteristic temperature dependences it is evident that the electron mobility is dominated by deformation potential scattering in the L_{1C} valleys, whereas it is dominated by strong intervalley scattering in the Δ_{1C} valleys as in silicon and GaP. Often in theoretical calculations of hot electron effects using, for example, Monte Carlo computer simulation, it is assumed that intervalley L scattering is weak as indicated by Ge while intervalley X scattering is strong as indicated by silicon. It is therefore reassuring to confirm this trend in a single material. It is also noticed that the electron effective mass in the Δ_{1C} valleys is somewhat higher than the measured masses in silicon. Fletcher and Pitt[9] found that a 50% increase would give reasonable fits to their high-pressure results and also the high-field calculations of Fawcett and Paige.[22] This hypothesis is also supported by our analysis of the ultrapure material.

From the series of experiments on ultrapure Ge, we have managed to determine the pressure coefficients for both the L_{1C} and the Δ_{1C} minima, the latter for the first time. The resulting pressure coefficients being

$$\frac{dE_L}{dP} = 4.8 \pm 0.2 \times 10^{-6} \text{ eV bar}^{-1} ,$$

$$\frac{dE_\Delta}{dP} = -2.4 \pm 0.4 \times 10^{-6} \text{ eV bar}^{-1} .$$

These values are independent of the energy separation, $\Delta E_{L\text{-}\Delta}$, at atmospheric pressure or the density of states of the minima. However, taking the density-of-states effective masses $m_L^* = 0.56$, $m_\Delta = 1.58$, and $m_V^* = 0.4$, which gave good agreement with the results of n-type Ge, resulted in best fits over the whole pressure range with $\Delta E_{L\text{-}\Delta} = 0.21 \pm 0.01$ eV and band $(L_{1C} - \Delta_{1C})$ crossover at 29 ± 2 kbar. The sub-band gap $\Delta E_{L\text{-}\Delta}$ is in good agreement with the value of 0.20 eV measured by Slykhouse and Drickamer.[34] It is interesting to note the unexpectedly large negative pressure coefficient $dE_\Delta/dP = -2.4 \times 10^{-6}$ eV bar^{-1}.

ACKNOWLEDGMENTS

The authors are considerably indebted to Dr. G. D. Pitt and Dr. D. Lancefield for valuable discussions and to Mr. B. J. Grunney, Mrs. V. Hinton, Dr. B. J. Sealy, and Dr. A. K. Saxena for technical assistance and help with some of the measurements. They are also grateful for financial support from the United Kingdom Science and Engineering Research Council (SERC).

[1] P. H. J. Miller and J. Taylor, Phys. Rev. **76**, 179 (1949).
[2] W. Paul and H. Brooks, Phys. Rev. **94**, 1128 (1954).
[3] M. I. Nathan, W. Paul, and H. Brooks, Phys. Rev. **124**, 391 (1961).
[4] A. Jayaraman and B. B. Kosicki, in *Proceedings of the Ninth International Conference on the Physics of Semiconductors, 1968* (Nauka, Leningrad, 1968), p. 947.
[5] W. Paul and G. L. Pearson, Phys. Rev. **98**, 1755 (1955).
[6] W. Paul, J. Phys. Chem. Solids **8**, 196 (1959).
[7] D. J. Wolford, H. Mariette, and J. A. Bradley, Inst. Phys. Conf. Ser. **74**, 275 (1985).
[8] G. D. Pitt, Contemp. Phys. **18**, 137 (1977).
[9] K. Fletcher and G. D. Pitt, J. Phys. C **4**, 1822 (1971).
[10] C. N. Ahmad, A. R. Adams, and G. D. Pitt, J. Phys. C **12** L379 (1979).
[11] L. J. Van der Pauw, Philips Res. Rep. **31**, 1 (1958).
[12] M. K. R. Vyas, G. D. Pitt, and R. A. Hould, J. Phys. C **6**, 285 (1973).
[13] R. Zallen and W. Paul, Phys. Rev. **134**, A1628 (1964).
[14] D. Long, Phys. Rev. **120**, 2024 (1960).
[15] D. L. Rode, Phys. Status Solidi B **53**, 245 (1972).
[16] B. A. Weinstein and G. J. Piermarini, Phys. Rev. B **12**, 1172 (1975).
[17] G. D. Pitt and J. Lees, Phys. Rev. B **2**, 4144 (1970).
[18] G. Dresselhauss, A. F. Kipp, and C. Kittle, Phys. Rev. **98**, 368 (1955).
[19] L. Eaves, R. A. Stradling, and R. A. Wodd, Proceedings of the Xth International Conference on the Physics of Semiconductors, Cambridge, 1970 (unpublished).
[20] P. P. Debye and E. M. Conwell, Phys. Rev. **93**, 693 (1954).
[21] F. J. Morin, Phys. Rev. **93**, 62 (1954).
[22] W. Fawcett and E. G. S. Paige, J. Phys. C **4**, 1801 (1971).
[23] M. Lax and J. L. Birman, Phys. Status Solidi B **49**, K153 (1972).
[24] M. Lax and J. J. Hopfield, Phys. Rev. **124**, 115 (1961).
[25] H. W. Streitwolf, Phys. Status Solidi **37**, K47 (1970).
[26] D. C. Herbert, W. Fawcett, A. H. Lettington, and D. Jones, in *Proceedings of the 11th International Conference on the Physics of Semiconductors, Warsaw, 1972*, edited by M. Miasek (PWN—Polish Scientific, Warsaw, 1972), p. 1221.
[27] B. N. Brockhouse and P. K. Iyenger, Phys. Rev. **111**, 747 (1958).
[28] W. A. Harrison, Phys. Rev. **104**, 1281 (1956).
[29] C. Herring and E. Vogt, Phys. Rev. **101**, 944 (1956).
[30] Masaharu Toyama, Mokoto Naito, and Akinobu Kasami, Jpn. J. App. Phys. **8**, 358 (1969).
[31] E. M. Conwell, Phys. Lett. **4**, 64 (1960).
[32] A. R. Adams and L. G. Shantharama, Physica B (to be published).
[33] F. J. Morin and J. P. Maita, Phys. Rev. **94**, 1525 (1954).
[34] T. E. Slykhouse and H. G. Drickamer, J. Phys. Chem. Solids **7**, 210 (1958).